PROPERTY INVESTIGATION OF MICROWAVE PROCESSED LITHIUM PHOSPHATE GLASS DOPED WITH FERRIC OXIDE

SHADO A. S; ALIU E.T; KENNETH-EMEHIGE C. A

Department of Glass and Ceramic Technology, School of Science and Computer Studies, The Federal Polytechnic Ado Ekiti, P.M.B 5351 Ado Ekiti, Nigeria

Corresponding author's email- shadoadeniyi@gmail.com

ABSTRACT

Microwave heating when compared to conventional showed rapid heating leading to shorter processing time, uniform temperature distribution, reduced energy consumption, improved material properties, finer or more controlled crystal structures or grain sizes and cost savings. In this study, $NH_4H_2PO_4$, Li_2CO_3, and $Ca(OH)_2$ (ACL) powders were mixed with and without iron dopant Fe_2O_3. The two variant mixtures (i.e., raw mixtures with and raw mixtures without dopant) were then subjected to microwave energy radiation. The samples were characterized by various methods of analytical methods. Microwave heating has no unmelted crystalline phase (i.e. raw material) left within the produced glass samples. Both compositions were able to form glass after experiencing glass transition temperature through microwave energy radiation for 15mins at a temperature of 956^0C. The connection between mixtures with and without dopant and degree of microwave absorption, and how they were influenced in glass formation were discussed. The FTIR showed the vibrational band of the samples with different structural change. SEM observations showed sample containing 1.03g wt% CaO, had a large columnar-shape rutile phase that appeared in the cross-section.

KEYWORDS: ACL, microwave energy, glass, $NH_4H_2PO_4$, Li_2CO_3, and $Ca(OH)_2$

1.0 Introduction

Doping is used to change a material, like glass resistivity and other properties. When certain elements, known as dopants or doping agents, are added to a chemical substance to change its original electrical or optical properties, the dopant atoms become absorbed into the crystal lattice. To change a glass's properties, such as conductivity, dopants like halides or sulfates are added to the host material. The salts such as AgI, NaI, NaF, NaCl, NaBr, KI, KF, LiI, LiF, LiCl etc. are added to the host glass matrix to produce mobile ion species Li+, Ag+, Na+, K+ etc. Numerous experiments have shown that the dopant salts do not interact with the glass' macromolecular chain. As a result, glasses are effective in dissolving metal ions. Diffusion and ion implantation are the two ways used in the process of doping, and a microwave ion source is used in the ion implantation step. In addition to its many other uses, microwave energy is now being used in a novel way for high-temperature material processing. Due to its quicker, cleaner, and more cost-effective procedures when compared to conventional methods, the use of this energy for material processing is becoming increasingly important. The ability of a substance to absorb microwave energy relies on its dielectric loss factor, frequency, and intensity. The Dielectric loss (loss tangent) should be strong enough to absorb microwave at a specified frequency at room temperature with the given/available microwave output (MW) power (Metaxas and Meredith,1983).

Raw materials used in glass making are broadly classified into three major groups, namely (1) glass formers (such as SiO_2, B_2O_3, P_2O_5, As_2O_5, GeO_2, *etc.*); (2) intermediate (such as Al_2O_3, PbO, BeO, TiO_2, ZrO_2) and (3) modifier (*i.e.*, alkali oxides, alkaline earth oxides and transition metal oxide). To give the batch of glass the required color and to remove air bubbles, small amounts of additional raw materials, referred to as colorants and fining agents, are added. Except for a few transition metal oxides, a few metal compounds, and a few other materials that contain water molecules in their composition, the majority of raw materials used to make glasses are poor microwave absorbers at room temperature. At room temperature and with low MW power, silica and commercial glass compositions are virtually transparent to microwave radiation. The research of glass and its raw materials' absorption at higher output power and room temperature falls under the

purview of this body of inquiry (Mishra, and. Sharma 2016, Clark and Folz 2000).

Unlike conventional heating, microwave heating offers shorter processing time, provides more uniform temperature distribution within the material, resulting in better control over the microstructure and properties of the glass. Reduces the overall energy consumption compared to conventional methods that may involve prolonged heating. It also influences the microstructure of the glass. It may lead to finer or more controlled crystal structures or grain sizes and improved material properties. Microwave processing equipment have cost savings in the long run.

Materials and Methods

Materials

2.1 Ammonium Dihydrogen Orthophosphate

Ammonium dihydrogen phosphate is defined with chemical names Ammonium dihydrogen phosphate, ammonium dihydrogen tetraoxophosphate, monoammonium monophosphate, ammonium dihydrogen orthophosphate. Chemical formula $NH_4H_2PO_4$, Formula weight 115.03, Colorless or white crystals, a white crystalline powder or granules. Ammonium phosphate ($NH_4H_2PO_4$) is produced by reacting phosphoric acid (H_3PO_4) with anhydrous ammonia (NH_3). By adding regular superphosphate or triple superphosphate to the mixture, ammoniated superphosphates are created. In fertilizer mixing plants, the generation of liquid ammonium phosphate and ammoniated superphosphates is regarded as a separate process.

2.2. **Method**

This study is experimental

2.3 ***Preparation of Materials***

A precise proportion of 82.82g, 5.186g, and 15.517g of each of the raw materials—ammonium dihydrogen phosphate ($NH_4H_2PO_4$), calcium hydroxide ($CaOH_2$), and lithium carbonate (Li_2CO_3—was accomplished in order to really produce glass. Due to the small size of the graphite pot, a reduction by five times the initial proportion was used to arrive at the final proportion, which was then weighed using a digital scale and combined to create a homogeneous, finer particle. To perform a doped fresh sample, ferric oxide Fe_2O_3 (1g) was additionally added. Also, the brick was drilled to create an opening for the graphite pot crucible and to enhance the heating rate (13 – 15◦C) microwave susceptors (SiC) were placed inside the insulation box.

Table 1: Glass composition

s/n	Materials	Orginal proportion(g)	Final proportion(g)
1	$NH_4H_2PO_4$	82.82	16.5
2	$CaOH_2$	5.186	1.03
3	Li_2CO_3	15.517	3.1
4	Fe_2O_3	1	0.2

Table 2: Glass composition and the melting condition

$NH_4H_2PO_4$,/ $CaOH_2$ / Li_2CO_3 ratio	Melting temperature (^oC)	Melting time (min)
16:1:3	956.8	15

2.4 ***Batch charging***

The homogeneous mixture of $NH_4H_2PO_4$ (16.5g), $CaOH_2$ (1.03g) and Li_2CO_3 (3.1g) was weighed, poured inside the small graphite pot crucible, place inside a covered insulating brick and finally charged into the microwave oven. The same proportion of $NH_4H_2PO_4$, $CaOH_2$ and Li_2O_3 was also mixed with the addition of Fe_2O_3 (0.02g) has another sample that was charged to determine the effect of ferric oxide in the glass after formation.

Figure 2: a fabricated kiln pot laced with silicon carbide and graphite pot crucible filled with the batch to be charged into the microwave oven.

2.5. ***Forming***

The batch as seen in figure 1 was place inside the microwave oven (thermocool HTMO 2380EG) 900W and was set to an irradiation time at exactly 15mins respectively for each sample. As the microwave was turned on, the rotating brick inside the oven helped to ensure uniform radiation. As soon as the time of irradiation was finished, the temperature created was measured using an infrared thermometer pointing to melt within the graphite pot, which assessed to 956.8O C. A tong was used to pour the molten glass from the graphite crucible pot into a graphite mold, which was then moved back into the microwave oven for annealing. The insulating box was then brought out. This process was used to create a glass and then repeated to create an iron-doped glass.

Figure 3. (a)(b)(c)

(a) After irradiation of 15mins and the insulating box brick brought out

(b) Tong pouring of the molten glass melt

(c) Final samples removed from the mold.

2.6. **Characterization of samples**

The comparing of the glass with an iron doped glass to determine the various properties of both glasses shall be done conducting the Fourier transmission infrared measurement (FTIR), optical transmittance, refractive index, x – ray refractive index (XRD), DSC and scanning electron microscopy SEM – EDS, Bulk density and chemical stability.

2.7. XRD

The samples were analyzed using X-ray diffraction spectrometer (XDS 2400H X-ray diffractometer equipped with a MiniFlex2^{+} goniometer and detector). The samples were oven-dried at 105^{0}C, crushed, milled and homogenized to powders of below 63 µm particle size. About 2g of each sample was placed on XRD's acrylic holder in readiness for analysis. Using XRD equipment ((XDS 2400H X-ray diffractometer equipped with a MiniFlex2^{+} goniometer and detector).) at CuK" radiation (λ=1.541838Å), 30 mA, 40 kV and 22 reflections, the samples were analyzed at 0-90^{0}C every 2 sec count time and 0.02^{0} step size.

2.8 Refractiveness

Refractive index, also called **index of refraction**, measure of the bending of a ray of light when passing from one medium into another. If *i* is the angle of incidence of a ray in vacuum (angle between the incoming ray and the perpendicular to the surface of a medium, called the normal) and *r* is the angle of refraction (angle between the ray in the medium and the normal), the refractive index *n* is defined as the ratio of the sine of the angle of incidence to the sine of the angle of refraction; i.e., $n = \sin i / \sin r$. Refractive index is also equal to the velocity of light *c* of a given wavelength in empty space divided by its velocity *v* in a substance, or $n = c/v$. The refractive index of the samples was measured at λ = 589.3 nm on a Abbé refractometer with the mono-bromo-naphthalene as a contact layer between the sample and prism of a refractometer by using sodium vapor lamp as the source.

3.0 RESULT AND DISCUSSION

Table 3 Refractiveness

Samples	Refractive index at 589.3nm
ACL	1.53
ACL (Doped)	1.51

Table 3 shows the refractive index of sample glasses with ACL sample having the highest reactive index of 1.53. This indicates both samples meet up eyeglasses standard refractive index.

Figure 4.1 - 4.2 displays FTIR reflectance spectra for all samples at room temperature from 650 to 4000cm−1. The spectra reveal the presence of phosphate tetrahedral, Li–O–Li bridging, octahedral vibration at 709–719, 903, 1261cm−1. The vibrational band appearing at 1259 cm−1 represents P = O asymmetric stretching for the PO_2 chain. The band appearing within 722 – 779cm−1 is due to symmetric stretching for P–O–P bridges (Dayanand et. al. 1996). The band at ~1830 has been shifted to 1978cm−1 for 3.1g of Li_2O. (Belkébir et. al. 1999). Asymmetric stretching of PO_3 groups in *(*PO4*)* − 3 units contributed the weak band at 1091cm−1 28 (Almieda et. al. 1980). Band at ~1142cm−1 is ascribed to the symmetric and asymmetric vibrations of P = O in PO_2 chain. The band appeared at ~918cm−1 is attributed to the asymmetric vibrational stretching modes of bridging oxygen of P–O–P bonds. The glasses studied at 3.1g Li_2O (ACL Fe doped) produced a different vibration this may be due to the structural changes associated with the decrease of PO_3 units in glass.

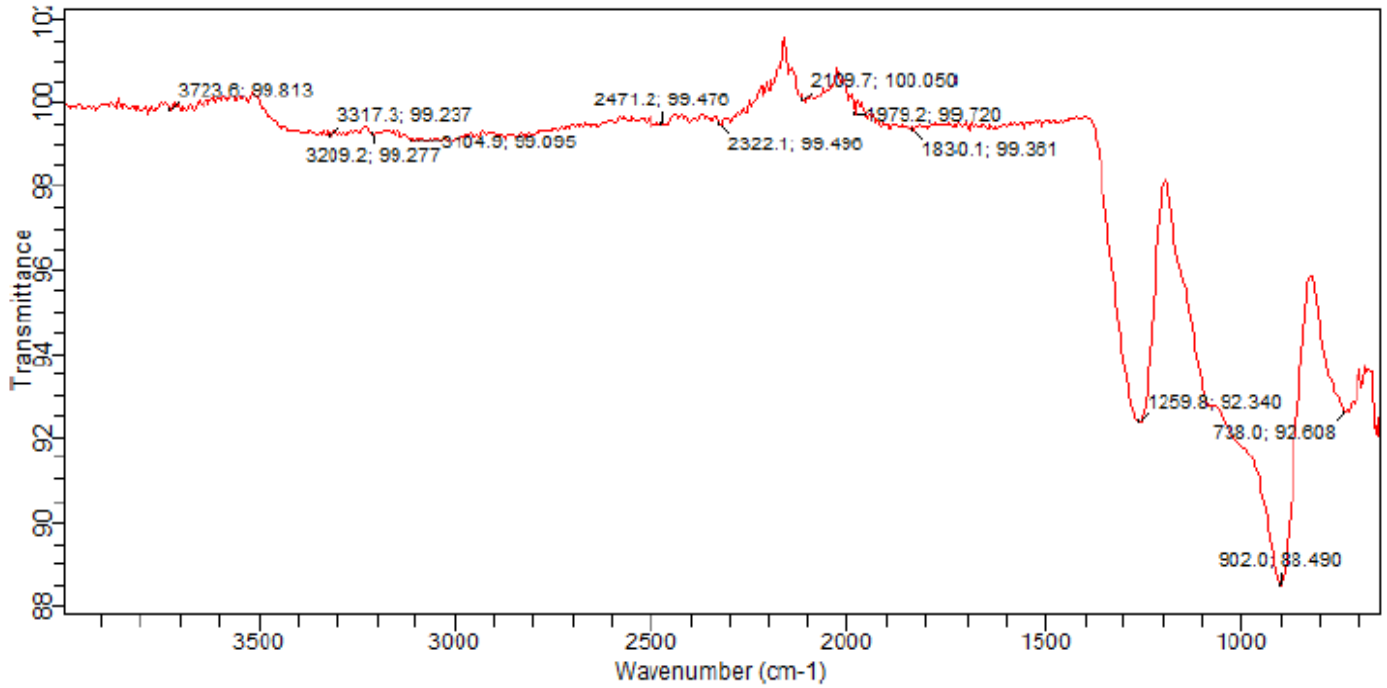

Figure 4: FTIR spectra of ACl Fe doped

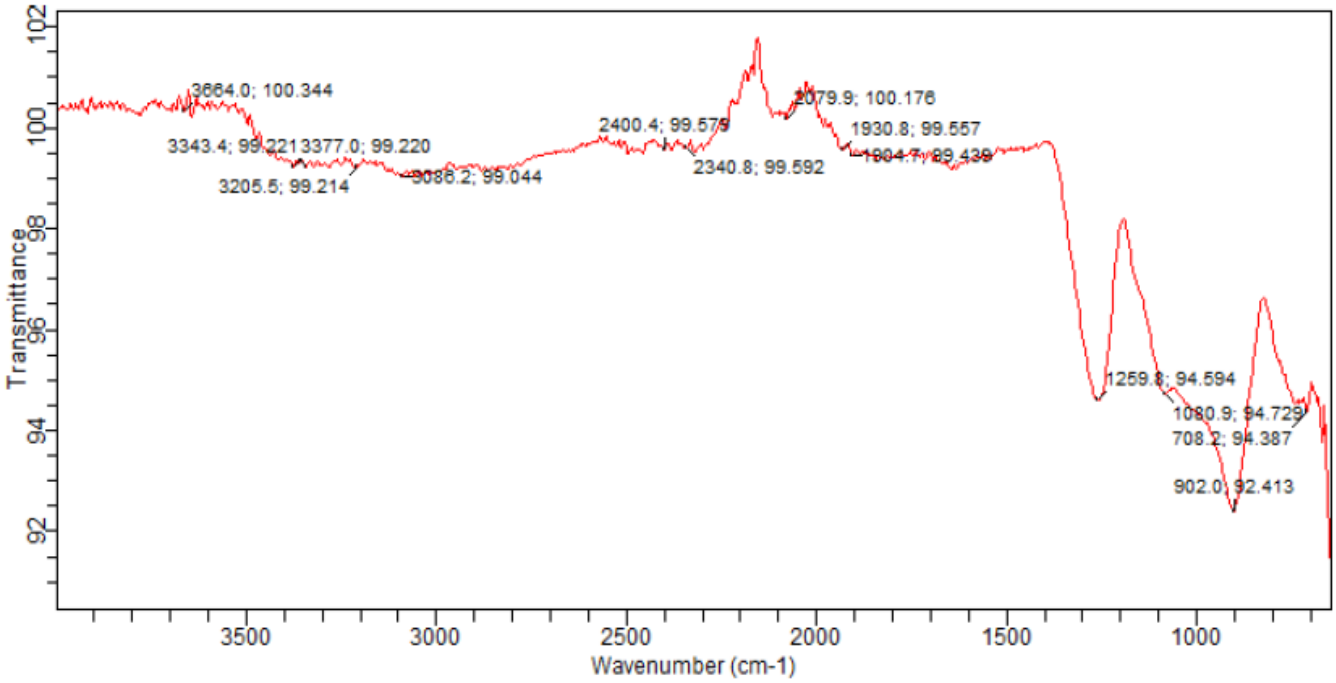

Figure 5: FTIR spectra of ACl Glass

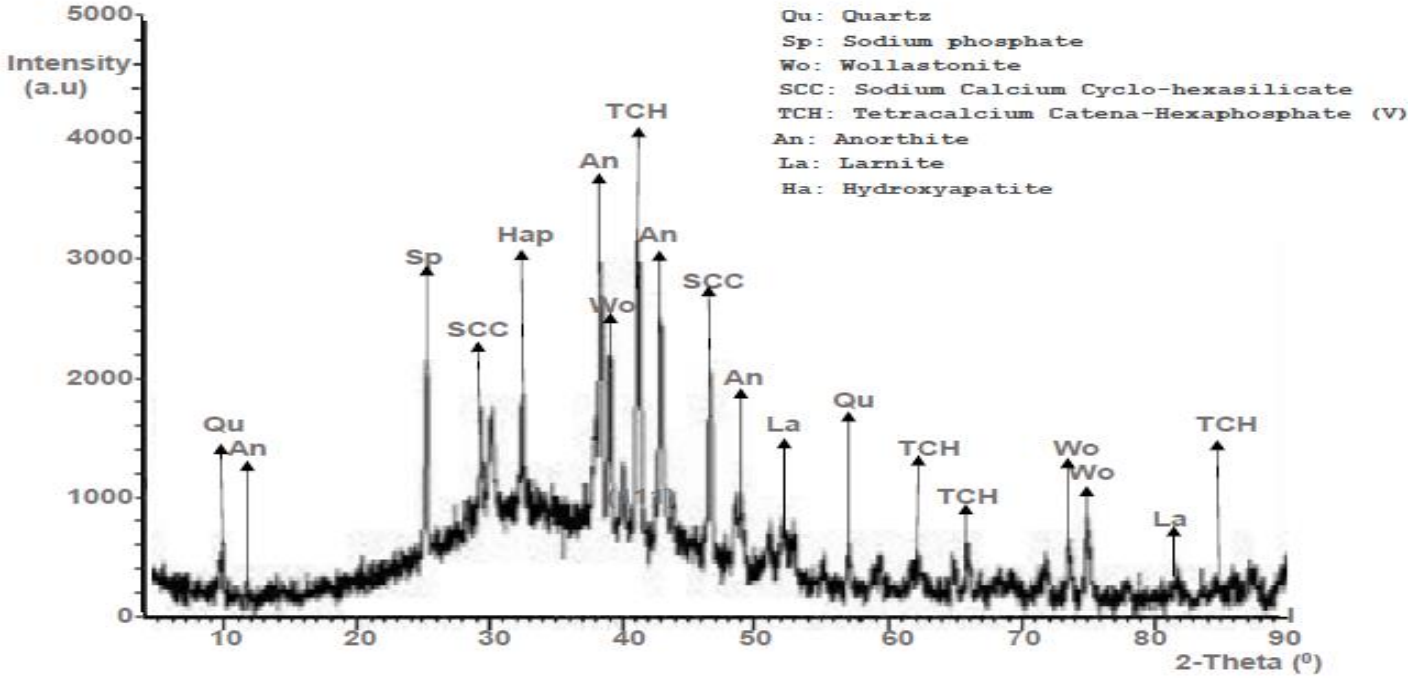

Figure 6: X-ray diffractograms of ACL glass sample

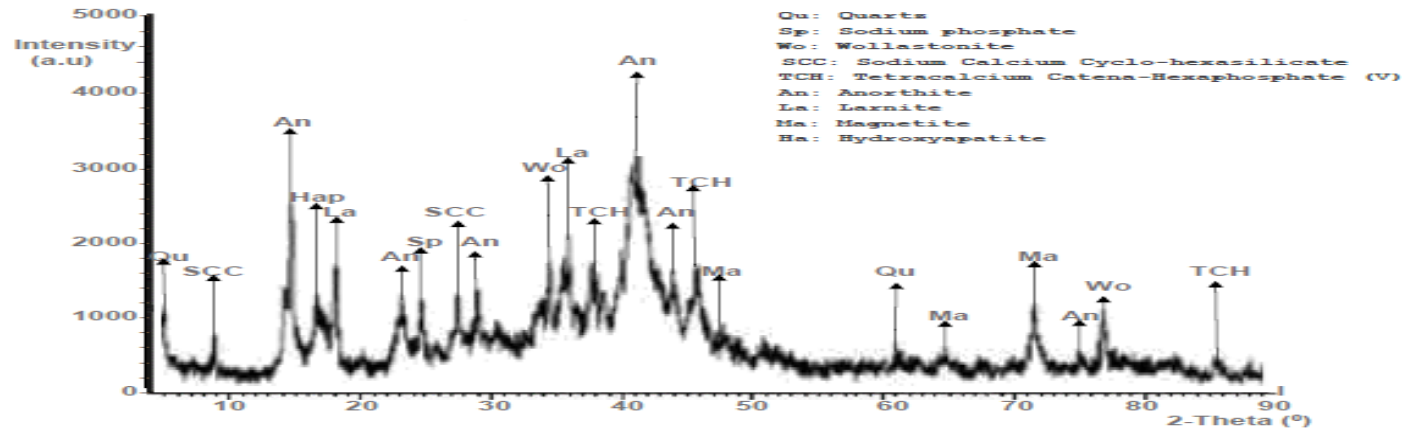

Figure 7: X-ray diffractograms of ACL iron doped glass sample

Figure 6 – 7 depicts X-ray diffractograms for ACL and ACL Fe doped glass samples. Observation of a broad hump centered around $2\theta = 25^{\circ}$ on the third peak and absence of any sharp peak, confirm amorphous nature of the sample ACL. This further demonstrates that the glass sample through microwave heating lost all of its unmelted crystalline phase (raw material).

In general, phosphate glasses with longer phosphate chains are more stable against devitrification. For example, (Yu et. al. 1997) reported that crystallization tendency of a complex Ca-phosphate glass increases with increasing Oxygen/Phosphate ratio as smaller phosphate anions are available to constitute the glass structure. (Crystallization tendency also depends on the nature of oxides used to modify the glass; oxides that strengthen the glass network, like Al_2O_3 and TiO_2, increase viscosity and reduce crystallization tendency compared to oxides like CaO and Na_2O.) According to (Zhang et. al. 2010), the addition of different oxides tends to decrease the temperature difference between Tg and Tx in iron doped phosphate base glasses, showing an increase in crystallization tendency with increasing Oxygen/Phosphate ratio (Jiangtao et. al 2018).

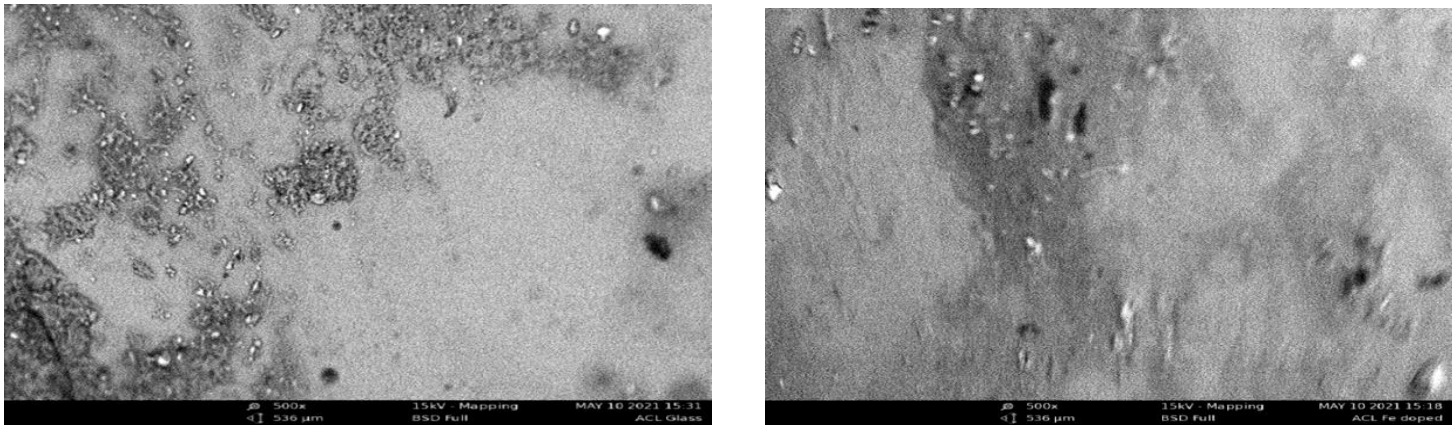

Figure 8: (a) SEM micrograph of ACL glass sample (b) SEM micrograph of ACL glass sample doped with Fe

SEM microstructure study revealed closed holes with good sphericity in every sample. Anatase crystals exhibit cubic, columnar, or needlelike morphologies, while precipitated rutile crystals have needle-like or columnar shapes, according to a substantial number of prior researches, including (Fiedberg et al. 1948). The SEM observations clearly show the size of the precipitated crystal (Figures 8-9).

3.1. Chemical stability properties

The qualities of water resistance and acid resistance make up the majority of the chemical stabilities of glass products. In this investigation, produced glass samples ACL and ACL Fe doped were completely submerged in water solution with pH values of deionized water (pH=7). Table 4 displays the mass variations of these samples. Table 4 shows that after a particular amount of time, samples immersed in water solution did not experience any noticeable mass alterations, and that these mass changes vary depending on the different Li_2O concentrations. The sample mass variation is more stable the more Li_2O is added. Due to the fact that the chemical stabilities of glass are mostly dependent on the movement of alkali ions, the mixed alkali effect may be used to explain this phenomenon (Conradt et. al. 1996, Conradt, 2008). A sufficient amount of Li+ fills in the gaps in the glass network structure and prevents the movement of large-radius ions like Na+ and K+, greatly reducing glass erosion by aqueous solutions and ultimately enhancing chemical stabilities. The gathering effect is exacerbated by excess Li+ present in the structure, which lowers chemical stabilities (Ashby and Gibson 1999).

Table 4. Effect of Li_2O on glass sample Chemical stability

Glass Samples	Bulk Density (g/cm^3)	Mass change in solution (Ph =7) (%)
ACL	2.46	+1.85
ACL Fe doped	2.52	+1.90

3.2. Comparison between refractive index and Bulk density

From the results, it is clear that ACL Fe doped with high bulk density has reduced refractive property due to atoms that is densely bound and so hinders light transmission, and that the opposite is true for ACL. Additionally, the ACL Fe doped has greater strength than the ACL despite having a larger bulk density (Karabulut et. al., 2002).

4. CONCLUSION

This study examines the effects of melting dry raw combinations of $NH_4H_2PO_4$, Li_2CO_3, and $Ca(OH)_2$. Following the addition of Fe_2O_3, the white color of the particle's changes to brown. The SEM morphology also reveals that all of the samples had closed pores with high sphericity. After a specific amount of time, samples submerged in water solutions exhibited minimal mass changes; however, these mass changes are dependent on the Li_2O concentrations. Microwave heating has the benefit of very quick processing times and energy conservation, which can be used to meet glass manufacturing specifications.

RECOMMANDATION

The following are recommended for future studies;

1. Produce phosphate glass with rightful doping agent for application such as bone regeneration, tissue repair and muscle repair.
2. Develop biocompatible material through unexpected structural modification exhibited by doping agent.
3. Helps to engage in commercial production of glass with low melting temperature material.

References

A.C. Metaxas, R.J. Meredith, (1983) *Industrial Microwave Heating* (The Institution of Engineering and Technology, London, United Kingdom,

Almieda RM and Mackenzie J D 1980 *J. Non-Cryst. Solids* 40 Belkébir A, Rocha J, Esculcas A P, Berthet P, Gilbert B, Gabelica Z *(*1999) *Spectrochim. Acta Part A* 55 1323

D.E. Clark, D.C. Folz, J.K. (2000) West, Processing materials with microwave energy. Mater. Sci. Eng. A 287(2), 153–158

Dayanand C, Bhikshamaiam G, Tyagaraju V J, Salegram M and Krishna Murthy A S R (1996) *J. Mater. Sci.* 31 1945

Fiedberg, A. L., Fischer, R. B. & Petersen, F. A. (1948) Effect of size and shape of titanium oxide crystals on spectrophotometric properties of titanium-bearing porcelain enamels. *J. Am. Ceram. Soc.*, 31 (9), 246–53.

Gibson LJ and Ashby MF. (1999) Cellular solids, structure and properties. Cambridge: Cambridge University Press,

Jiangtao Cui, Hongli Wen, Shengjie Xie, Wei Song, Ming Sun, Lin Yu, Zhifeng Hao, (2018), Synthesis and characterization of aluminophosphate glasses with unique blue emission, Materials Research Bulletin, Volume 103,

Karabulut, Mevlüt, G. K. Marasinghe, Chandra S. Ray, D. E. Day, G. D. Waddill, C. H. Booth, P. G. Allen, J. J. Bucher, D. L. Caulder, and D. K. Shuh. (2002) "An investigation of the local iron environment in iron phosphate glasses having different Fe (II) concentrations." Journal of non-crystalline solids 306, no. 2 (2002): 182-192.

L. Zhang, L. Ghussn, M.L. Schmitt, E.D. Zanotto, R.K. Brow, and M.E. Schlesinger. (2010) "Thermal stability of glasses from the Fe4(P2O7)3–Fe(PO3)3 system." Journal of Non-Crystalline Solids 356, no. 52 (2010): 2965-2968.

R. Conradt, and P. Geasee. (1996) "An improved thermodynamic approach to the stability of multi-component silicate glasses in aqueous solutions." Berichte der Bunsengesellschaft für physikalische Chemie 100, no. 9 (1996): 1408-1410.

R. Conradt. (2008) "Chemical durability of oxide glasses in aqueous solutions: A review." Journal of the American Ceramic Society 91, no. 3 (2008): 728-735.

R.R. Mishra, A.K. Sharma, (2016) Microwave-material interaction phenomena: heating mechanisms, challenges and opportunities in material processing. Compos. A Appl. Sci. Manuf. 81, 78–97

X. Yu, D.E. Day, G.J. Long, and R.K. Brow. (1997) "Properties and structure of sodium-iron phosphate glasses." Journal of non-crystalline solids 215, no. 1 (1997): 21-31.